Journal of the European Ceramic Society 17 (1997) 773–780

PII: S0955-2219(96)00165-5
0955-2219/97/$17.00

SiC Particle Reinforced Oxynitride Glass: Processing and Mechanical Properties

Benoît Baron,[a] Thierry Chartier,[b] Tanguy Rouxel,[b] Patrick Verdier[a] & Yves Laurent[a]

[a]Laboratoire de chimie des matériaux (URA CNRS 1496), Université de Rennes 1, Avenue du Général Leclerc, F-35042 Rennes, France
[b]Laboratoire de matériaux céramiques et traitements de surface (URA CNRS 320), ENSCI, 47, Avenue Albert Thomas, F-87065 Limoges, France

(Received 13 December 1995; revised version received 1 August 1996; accepted 5 August 1996)

Abstract

After optimization of the processing route, the mechanical properties of the composites were evaluated with varying particle sizes and volume fractions of reinforcement. The best dispersion of the particles in the composite was obtained by using attrition milling followed by spray-drying; nevertheless, ball-milling led to satisfactory results for particle sizes higher than 3 μm. Elastic moduli, hardness and fracture toughness increase with the volume fraction of SiC. Fracture strength increases with both decreasing particle size and increasing volume fraction to reach 400 MPa for a glass matrix composite containing 47 vol% of SiC with 1 μm average particle size. A further improvement is achieved by crystallizing the matrix. © *1997 Elsevier Science Limited. All rights reserved.*

1 Introduction

Glasses and glass-ceramics offer a unique combination of structural properties. Their advantages over ceramics are their suitability for viscoplastic forming technique, i.e. at relatively low temperature, and their infinite numbers of compositions which give the possibility to continuously modify their properties.

In oxynitride glasses, some of the divalent oxygen atoms are replaced by trivalent nitrogen. The result is a significant increase of the mechanical and physical properties (elastic modulus, hardness, fracture toughness, strength, viscosity.)[1–5]

However these glasses remain very brittle, with fracture toughness of the order of 1 MPa $\sqrt{m}$. A well-known method to increase the fracture toughness and resistance of bulk ceramics or glasses is the addition of a second phase. Particulate reinforcement has the potential of yielding improvements in strength and toughness[6] at little or no additional cost without losing the viscoplastic forming ability.

Therefore the processing route must be carefully designed to lead to a dense and homogeneous microstructure. To achieve microstructure homogeneity, it is recognized that the process before thermal treatment and in particular the mixing of the powders is very important.

The present study has been devoted to the preparation of an oxynitride glass reinforced by SiC particles. The potential of this composite for structural uses and its viscoplastic forming ability have already been demonstrated in previous studies.[7,8] Here, after optimization of the processing route, the development of the mechanical properties with the size and the volume fraction of the particles, which is of major interest for designing particulate composites, was evaluated. A further improvement of the materials can be achieved through a post-forming crystallization treatment.

2 Materials and Experimental Procedures

The different processing steps concerning the fabrication of the composites are illustrated in Fig. 1.

2.1 Starting materials

The matrix is an oxynitride glass with stoichiometric composition $Y_{0.124}Mg_{0.160}Si_{0.414}Al_{0.302}O_{1.4}N_{0.151}$. This glass presents a high glass transition temperature (863°C measured by dilatometric analysis) and a good potential for crystallization control.[8,9] It can be easily prepared by heating up to 1600°C under nitrogen atmosphere a mixture of Y_2O_3 (Rhône-Poulenc, France), MgO (light MgO, Prolabo, France), amorphous SiO_2 (Quartz et Silice,

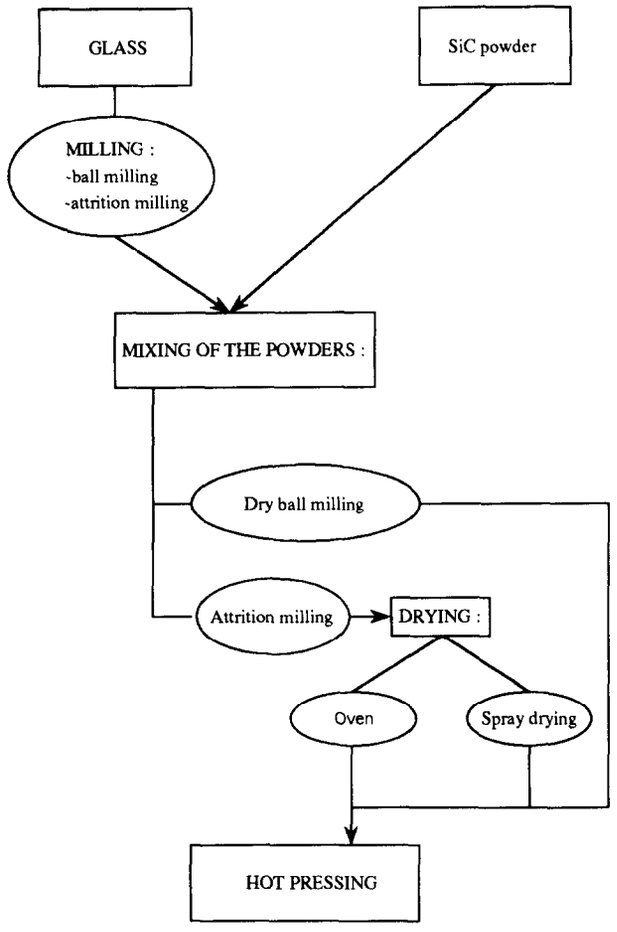

Fig. 1. Different ways of fabrication of the composites.

France), α-Al_2O_3 (Baikowski, Annecy-France) and AlN (grade A, H. C. Starck, Germany) powders with a purity of at least 99%, and subsequent quenching. Some properties of the glass are given in Table 1.

The chosen reinforcement is silicon carbide (SiC) powder. Easily available and cheap, this material of high mechanical performance possesses a coefficient of thermal expansion lower than and close to that of the glass (crystallized or not) and a high value of Young's modulus which are key conditions for obtaining a good reinforcement.[10,11] We used various grades of α or β-SiC. α-SiC are commercial powders which are approximately monodispersed grades UF10, Carborex BWF90, BWF800 and BWF1200 from Lonza, and grades Carborundum 37 and 51 μm from Prolabo). The β-SiC prepared in the laboratory (Si and C powders heated at 1800°C under nitrogen atmosphere), has a greater dispersion around the mean particle size.

2.2 Milling of the glass

In order to have the possibility of obtaining a good dispersion of the SiC particles in the glass matrix, the glass powder must be of a smaller particle size than the average size of the free spaces between the reinforcement particles in a well-dispersed composite. Indeed the largest particles of glass would not be broken down during hot pressing and such particles would then retain approximately their original size and then represent inhomogenities in the final composite. Fullman[12] calculated the mean free path, $<d>$, between the surfaces of spherical particles of uniform radius, R, statistically distributed throughout a matrix:

$$<d> = 4R(1 - f_p)/3f_p \quad (1)$$

where f_p is the volume fraction of the particles. $<d>$ can represent the average size of the free spaces between the particles. Table 2 gives the values of $<d>$ for the different composites prepared if we assume that monodispersed SiC powders are used.

Two techniques have been used for the milling of the glass. The first one is dry ball milling followed by sieving (20 μm) to obtain a mean particle size of 9 μm. The second one is attrition milling using water with a dispersant (1 wt% Darvan C, Vanderbilt Co., Norwalk, USA). After attrition milling (14 h at 450 rpm with zircon balls, 1 to 1·5 mm in diameter) the mean particle size decreases down to 1·6 μm. The suspension is then dried in an oven at 110°C.

2.3 Mixing of the glass and SiC powders

Compositions containing 5, 10, 20, 28, 40 and 47 vol% of various SiC powders were prepared. After weighing of the two powders in the desired proportions, the homogenization of the particles in the matrix was performed by mixing the glass and SiC powders. The distribution of the SiC powder in the composite will depend on the homogeneity of this mixture.

Two mixing techniques were used to disperse the particles in the matrix, namely dry mixing of the two powders by dry ball milling for 10 min (longer times do not change anything), and attrition milling in water with a dispersant (1 wt% of Darvan C) for 30 min. In this latter case, the drying technique of the suspension may influence the state of agglomeration of the dried powder. Characteristics of agglomerates (morphology, mean

Table 1. Glass and silicon carbide physical properties

	$\rho(g/cm^3)$	$\alpha(10^{-6}°C^{-1})$	$H_v(GPa)$	$\sigma_r(MPa)$	$K_{Ic}(MPa\sqrt{m})$	$E(GPa)$	$G(GPa)$	ν
Glass	3·18	6·5	8·3	162	1·2	134	50	0·28
Sic[a]	3·21	4·0	21·6	450	3·5	420	180	0·16

[a]Data from "Céramiques et composites" Tarbes, France, CCSiC-100.

Table 2. Influence of particle size and of the volume fraction of the SiC powder

Sample	ρ(*g/cm³*)	E(*GPa*)	G(*GPa*)	*v*	H_v(*GPa*)	K_{1c}(*MPa* $\sqrt{m}$)	$<\sigma_1>$(*MPa*)	σ_{max}(*MPa*)	<d>(μm)	a_c(μm)
5Sα6B	3·19	144	57	0·27	9·1	1·7	184	190	76	21
10Sα6B	3·19	150	59	0·27	9·6	1·8	217	218	36	17
20Sα6B	3·19	171	68	0·26	10·2	2·2	225	260	16	24
28Sα6B	3·21	193	78	0·24	10·7	2·6	251	293	10·3	27
40Sα6B	3·20	216	88	0·23	11·5	2·8	317	346	6	20
28Sα3B	3·21	193	77	0·26	10·4	2·7	267	340	5·2	26
28Sα15B	3·20	190	76	0·26	9·7	2·7	218	229	26·6	38
28Sα31B	3·20	—	—	—	—	—	173	182	53·1	—
28Sα150B	3·20	188	74	0·26	—	—	86	105	257·1	—
47Sα1AS	3·09	210	86	0·23	9·4	3·3	390	396	0·8	17
47Sα15B	3·20	221	90	0·23	11·1	3·1	271	280	11·7	33
47Sα31B	3·20	236	95	0·24	11·0	—	203	222	23·4	—
47Sα150B	3·20	238	97	0·23	—	—	106	115	112·8	—

<*d*> represents the average distance between the surfaces of the particles after Fullman [eqn (1)], and a_c the critical defect size calculated after eqn (2').

size, roughness of the surface) greatly influenced the arrangement of the particles, and thus the density in the green state and the homogeneity of the microstructure. Two ways of drying were compared: conventional drying in an oven at 110°C and spray drying with addition of a binder (3 wt% of PVA) in a laboratory spray-drier (Büchi 190 - Mini Spray Dryer, Switzerland).

2.4 Preparation of composites

Composites were obtained by hot pressing of the mixtures. In a earlier study,[9] the different parameters of the hot pressing were optimized in order to obtain full density with a maximum volume fraction of SiC. In the present study, the crystallization of the matrix has not been investigated in detail in order to limit the study to the influence of the mixing technique and of the SiC particle size and volume fraction. Figure 2 shows the hot pressing cycle.

The different grades and processing routes are listed in Table 3.

2.5 Characterization

The particle size distributions were determined by an X-ray granulometer (Sedigraph 5100, Micromeretics Inst. Co. GA, USA) and controlled by SEM image analysis. The density of the composites, after hot pressing, was measured by the Archimedes' method in water. Microstructural features were observed by optical microscopy on polished samples. Hardness and fracture toughness were measured by means of Vickers indents, the mode 1 fracture toughness K_{1c} was calculated from the equation of Marshall *et al.*:[13]

$$K_{1c} = 0{\cdot}036\, E^{0{\cdot}4} P^{0{\cdot}6} a^{0{\cdot}8} c^{-1{\cdot}5}$$

where E (Pa) is Young's modulus, P (N) is the load applied on the indent, a (m) is half the length of the indentation diagonal and c (m) is half the crack length. Experimental values of Young's modulus were used for this calculation. Preliminary tests were performed to determine the minimum load above which the median crack system

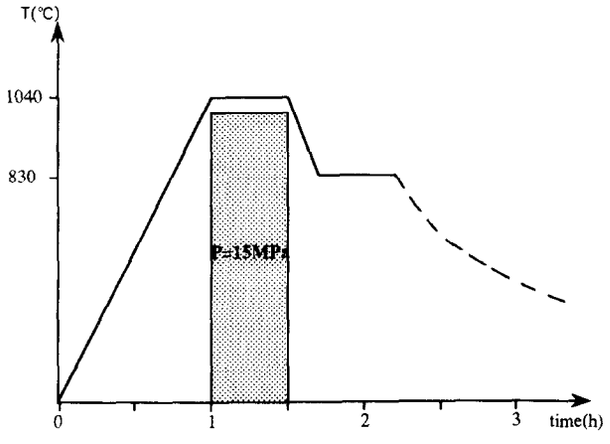

Fig. 2. Hot pressing cycle.

Table 3. Sample preparation

Samples	*SiC powder*	*vol% SiC*	*Mixing/drying method*
5Sα6B	α-SiC 6 μm	5	ball milling
10Sα6B	α-SiC 6 μm	10	ball milling
20Sα6B	α-SiC 6 μm	20	ball milling
28Sα6B	α-SiC 6 μm	28	ball milling
40Sα6B	α-SiC 6 μm	40	ball milling
28Sβ6B	β-SiC 6 μm	28	ball milling
28Sβ6A0	β-SiC 6 μm	28	attrition/dried in oven
28Sβ6AS	β-SiC 6 μm	28	attrition/spray drying
28Sα15B	α-SiC 15 μm	28	ball milling
28Sα31B	α-SiC 31 μm	28	ball milling
28Sα150B	α-SiC 150 μm	28	ball milling
47Sβ6B	β-SiC 6 mm	47	ball milling
47Sβ6AS	β-SiC 6 μm	47	attrition/spray drying
47Sα1AS	α-SiC 0·5 μm	47	attrition/spray drying
47Sα15B	α-SiC 15 μm	47	ball milling
47Sα31B	α-SiC 31 μm	47	ball milling
47Sα150B	α-SiC 150 μm	47	ball milling

The notation refers to (i) the amount of SiC(28 or 47 vol%); (ii) the SiC grade (α or β); (iii) the mean SiC particle size (0·5, 3, 6, 15, 31, 150 mm); (iv) the mixing method (B: ball milling and A: attrition milling) and (v) the drying method after attrition milling (O: oven and S: spray drying).

prevails (rather than the Palmqvist one)[14] and to assess the upper limit for the load before chipping of the indent occurs. A load of 10 kg was selected and the dwell time at peak load was 30 s. Each specimen was indented 10 times on mirror surfaces.

The fracture strength was measured from three-point bend experiments using three specimens [3(height) × 4(width) × 25 mm^3 rectangular bars] for each grade, with a cross-head speed of 0·5 mm min^{-1}. Young's and shear (G) moduli were determined by means of an ultrasonic technique, with 10 MHz piezoelectric transducers:

$$E = \rho\,(3V_l^2 - 4V_t^2)/(V_l^2/V_t^2 - 1);\ G = \rho V_t^2$$

where ρ is the specific mass, V_l is the longitudinal wave velocity and V_t is the transversal wave velocity. Poisson's ratio is then calculated from: $\nu = (E/2G) - 1$. The accuracy of this technique is better than 1 GPa.[15]

Residual stresses in the SiC particles resulting from thermal contraction mismatch with the matrix were measured by X-ray diffraction. The X-ray source is a chromium anticathode (λ = 0·2291 nm) and the detection is done with a linear detector equipped with a vanadium filter. All the samples were polished using the same route until 1 μm.

The X-ray spectra of the composites are compared to the spectrum of the starting silicon carbide powder. Measurements of the shift of the peak corresponding to the {2 0 2} plane of 6H SiC (major phase in the present materials) were used for the calculation. The normal stress σ_{33}, where the x_3 axis is perpendicular to the surface, was taken equal to zero, and the radiocrystallographic elastic constant are replaced by the macroscopic values (see Table 1). The hydrostatic stress, defined by $\sigma_H = (\sigma_{11} + \sigma_{22} + \sigma_{33})/3$, has been considered as indicative of the pressure in the particles.

3 Results and Discussion

3.1 Influence of the mixing method of the powders

Samples containing 28 vol% of β-SiC with a mean particle size of 6 μm were prepared (Table 3) by dry ball milling (28Sβ6B), or by attrition milling followed by drying in an oven (28Sβ6AO) or by spray drying (28Sβ6AS).

Figure 3 shows the different microstructures obtained depending on the dispersion method for these three grades. The dispersion observed in Fig. 3(a) is not good. The Fullman equation (eqn (1)) does not give a significant result in the case of a too large dispersion of the particle sizes (i.e.

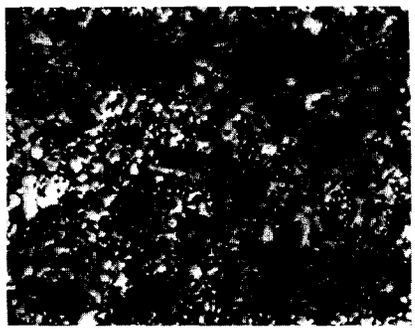

Picture a :
ball-milling

Picture b :
attrition and oven

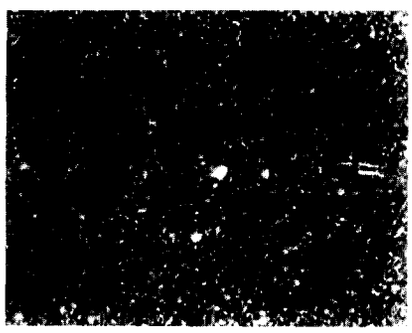

Picture c :
attrition and spray-drying

Fig. 3. Influence of the mixing method on the distribution of the particles in the glass matrix. Optical microscope observation.

β-SiC). Attrition milling leads to a more intimate mixture of the two powders and a more homogeneous microstructure than ball milling. But the drying route seems to be very important in the case of attrition milling. When the suspension is dried in an oven, glass agglomerates with large size and shape distributions are formed. These agglomerates leads to a poor arrangement of the particles in the die, the green density is low. These glass agglomerates were not broken during compaction and the SiC particles' distribution in the glass matrix was not homogeneous. The more homogeneous microstructure was achieved by spray drying.

As expected, the better the SiC dispersion in the matrix, the higher the mechanical strength. Best results were obtained for attrition milling and

Table 4. Influence of the dispersion on the mechanical properties

Sample	*Mixing/drying method*	E (*GPa*)	σ_r (*MPa*)	K_{Ic}(*MPa* $\sqrt{m}$)
28Sβ6AO	Attrition/dried in oven	190	273	2·6
28Sβ6B	Ball milling	185	286	2·3
28Sβ6AS	Attrition/spray drying	185	308	2·5

spray drying (Table 4) which leads to more homogeneous microstructure with smaller compaction defects and thus smaller critical defects. Young's modulus is not affected because this property depends only on the volume fraction of the two constituents when the composites are fully densified.

The samples containing 47 vol% of the same SiC grade prepared by ball milling and attrition milling associated with spray drying showed that this last method favours the densification of the composite. The samples obtained after ball milling present a density of 2·9 g/cm^3 while that obtained after attrition and spray drying has a density of 3·12 g/cm^3. The theoretical density calculated using the rule of mixtures is 3·21 g/cm^3. The glass and SiC powders are more intimately mixed by attrition milling and then there is less contact between SiC particles, leading to an easier flow of the glass during hot-pressing. In addition, as regards die pressing which was used in this study, the spherical morphology and the smooth surface of the soft spray-dried granules confer better properties for filling the die and for pressing. The green density was thus higher when spray drying was used.

3.2 Influence of the SiC particle size and volume fraction

Composites containing from 5 to 40 vol% of 6 μm SiC and two series containing respectively 28 and 47 vol% of SiC with grain sizes varying from 1 to 150 μm were prepared. Except for the sample containing very fine grain size (47Sα1AS), which requires attrition and spray drying to achieve correct dispersion and density, all the samples were prepared by ball milling (Table 3).

The mechanical properties of these composites are summarized in Table 2. Results show that except for the composite prepared with the 1 μm SiC powder, which could not be fully densified, all grades have near theoretical densities between 3·20 and 3·21 g/cm^3. Therefore, little change in the elastic modulus is observed through a series of materials with given SiC vol%. The increase in elastic modus resulting from the increase of the SiC vol% (f_p) agrees well with simple predictions for two-phase materials such as the Voigt and Reuss models for the shear moduli (Fig. 4). The

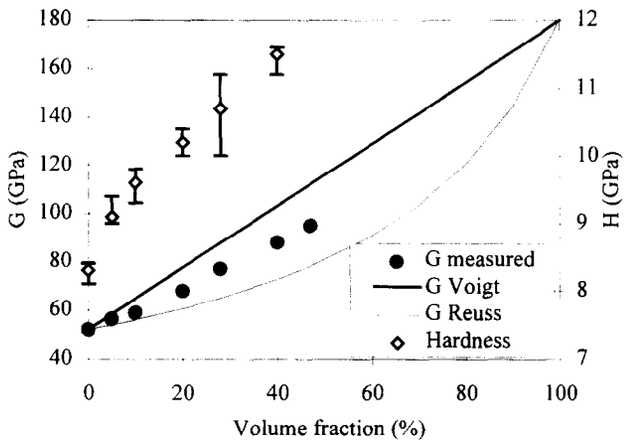

Fig. 4. Shear modulus and hardness as a function of SiC volume fraction.

slight decrease in Poisson's ratio results from a much lower Poisson's ratio for the particles than for the glass. The same conclusion can be drawn for the increase in hardness as f_p increases from 5 to 40 vol%.

As predicted by Evans[16] and observed by Swearigen *et al.*,[17] we observe here an increase of fracture toughness (Fig. 5) with increasing addition of higher-modulus particles in a lower-modulus matrix and no significant dependence on the particle size.

More important is the incidence of the particle size and volume fraction on the fracture strength, with a remarkable increase in strength with an increasing volume fraction and a decreasing particle size (Figs 5 and 6). Different mechanisms might be invoked to explain the dependence of

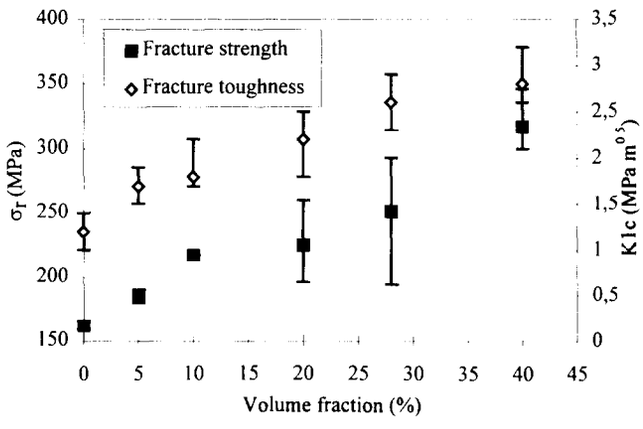

Fig. 5. Fracture strength and fracture toughness as a function of SiC volume fraction.

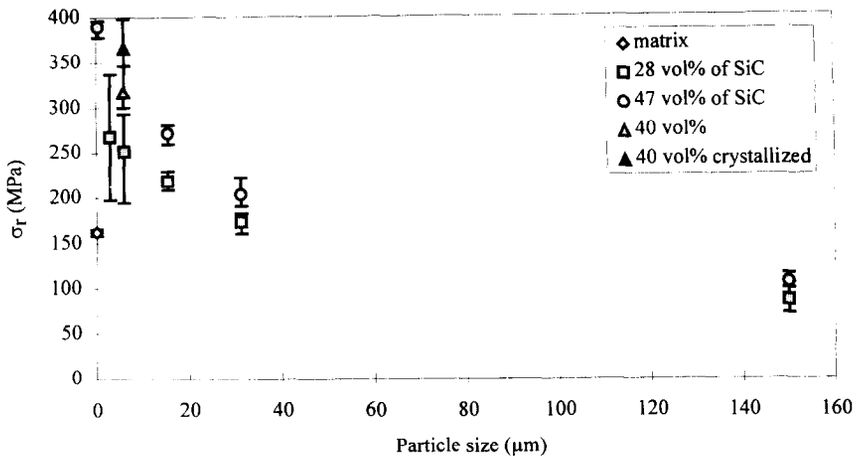

Fig. 6. Fracture strength as a function of the particle size.

the mechanical properties on these parameters. Changes in the second-phase characteristics might affect the critical flaw size which initiates fracture, the composite's Young's moduli and the residual stresses that develop upon cooling.

The increase in strength with the reduction of the critical flaw size can be visualized as a direct consequence of the Irwin relationship:

$$\sigma_r \propto K_{Ic}/\sqrt{a_c} \qquad (\propto: \text{proportional}) \qquad (2)$$

where a_c is the critical flaw size of the composite. A simple estimation of a_c can be obtained by assuming that fracture initiates at a surface flaw under a homogeneous tensile stress parallel to the surface, further neglecting any residual stress effect. In this case the expression for a_c becomes:

$$a_c \approx K_{Ic}^2/4\sigma_r^2 \qquad (2')$$

First of all, it must be underlined that the experimental value for K_{Ic} is certainly closely related to the technique. Slightly lower values were obtained by chevron notched method in the same materials. Hence, values for a_c are presumably slightly overestimated. For instance, K_{Ic} values of 1·2, 2·1 and 2·5 MPa $\sqrt{m}$ were measured by the chevron notched method for the matrix, a 28 vol% SiC composite (28Sα6B) and a 40 vol% SiC composite (40Sα6B) respectively.[18] This would correspond to initial flaw sizes of approximately 14, 18 and 16 μm respectively. However, for sake of comparison, K_{Ic} values obtained from indentation will be further used.

Identification of a_c with a characteristic distance of the microstructure is not straightforward. Typical approaches are those where a_c is assumed to scale with the interparticle distance or with the particle size. But first we will consider another possibility; a_c could be a flaw of the matrix like, for example, residual porosity. To examine this hypothesis we must either find the initiation of the rupture to know if it began on a particle or on a flaw of the glass, or find flaws existing in the composites but not in the glass. Scanning electron microscope observations fail to evidence such processing flaws. However, it is likely that the characteristics of the flaws depend on the particle radius because composites with the smallest particles are more difficult to densify and then contain some residual porosity.

Hasselman and Fulrath[19] proposed that, at relatively high volume fraction or small particle size, the flaw size is represented by the mean free path $<d>$ between particles. Values for $<d>$ are given in Table 2 from the expression derived by Fullman [eqn (1)] (a monodispersed SiC particle size distribution is assumed for this calculation). Using eqn (2') we have calculated the values of critical flaw for the composites (Table 2). In the series containing various volume fractions of 6 μm α-SiC, the values of a_c remain approximately constant despite a very large discrepancy of $<d>$. Thus in our case, a theory based on a direct scaling between $<d>$ and a_c does not give a realistic description of the fracture behavior.

Lange[20] measured the fracture energy and fracture strength of different sodium borosilicate glass–Al_2O_3 composites and calculated the corresponding values of a_c. He concluded that a_c scales with the particle radius.

Re-examining the results of Hasselman and Fulrath, Borom[21] considered that in such composites with rigid reinforcement the constituents share the applied load in proportion to their elastic modulus. It follows that the strain (ε) is the same in all the constituents, including the total system ($\varepsilon_c = \varepsilon_m = \varepsilon_p$), and then he wrote that:

$$\sigma_c = (E_c/E_m)\sigma_m \qquad (3)$$

Replotting the data of σ_r of Hasselman and Fulrath versus volume fraction and comparing the series of points obtained for each particle size with the curve calculated from eqn (3) where the second-phase volume fraction is implicitly taken

into account through the ratio E_c/E_m, he established that these series of experimental points could be fitted by equations of the same form with varying values of σ_m. These values of σ_m are all lower than the real fracture strength of the matrix and the bigger the particle size, the smaller is the value of σ_m necessary to fit the data. He concluded that the particles create flaws in proportion to their diameter. He found values of a_c approximately three times larger than the particle diameter. He explained the possibility of creation of such flaws by the stresses due to thermal contraction mismatch between the two phases.

Considering the values of a_c in the 6-μm α-SiC or 15-μm α-SiC series (Table 2), we could assume that such a theory is suitable. We can remark here that the critical flaw size of the composites seems to get no smaller than the value found for the 6-μm series. This value corresponds approximately to the critical flaw size of the glass (14 μm). This could mean that the addition of particles cannot reduce the original critical flaw size of the matrix.

These remarks, consistent with the earlier conclusions of Frey and Mackenzie,[20] lead to attribution of the increase in fracture strength with increasing volume fraction of particles (Fig. 5) to the resultant increase of Young's modulus.

After consideration of the effect of volume fraction and particle size on the size of the critical defect, we must consider the influence of the residual stresses developed upon cooling because of thermal contraction mismatch of the two phases.

Selsing[22] calculated the residual stress in the case of a spherical particle in an infinite matrix:

$$\sigma_i = -P(R/r)^3 \text{ with } P = (\alpha_m - \alpha_p)DT/((1 + \nu_m)/E_m + (1 - 2\nu_p)/E_p) \quad (4)$$

where σ_i is the radial stress in the matrix, R is the particle radius, r is the distance from the centre of the particle and α_m, α_p, E_m, E_p, ν_m and ν_p are respectively the coefficient of thermal expansion, Young's modulus and the Poisson's ratio of the matrix and of the particle. P represent the hydrostatic pressure. In the case of a particle embedded in an infinite matrix, the stress varies according to $(R/r)^3$. In our case for high volume fraction or small particle size the stress and strain fields surrounding the particles interact with each other. We can assume that this creates a state of variable compressive and tensile stress throughout the matrix with maxima near the particles and minima in the median plane between two particles. The values of these minima would depend on the distance between the median plane and the surfaces of the interacting particles which decreases with increasing volume fraction and particle size. These observations show the possibility of dependence of the internal stress field in the matrix with volume fraction or particle size.

Compiling the results obtained by different authors[11,23,24] for such composites, Nadeau and Dickson[10] showed that the effects of internal stresses resulting from contraction mismatch could vary with the particle size. They concluded that in the case of $\alpha_m > \alpha_i$ three domains of behaviours exist. For particles of 300 μm contraction mismatch can reduce the strength[24] because of precracking of the matrix around the particles. At the opposite, for composites containing 10-μm particles,[23] the best reinforcement possibilities are obtained for $\alpha_m > \alpha_i$. The transition between these two regimes occurs for particles 20–40 μm in size.[17,23] For such sizes there is little effect of contraction mismatch on the reinforcement effect. The comparison of the reinforcement effect measured in our materials corresponds exactly with the three domains of behaviour determined by Nadeau and Dickson.

The residual stresses in the SiC particles were measured in some of the composites to evidence their possible dependence on the volume fraction and size of the particles (Table 5). All the measurements give negative values of normal stress inside particles, consistent with the compressive stresses predicted from the thermal contraction mismatch between the particles and the matrix. Calculated values for σ_H are probably slightly underestimated. To some extent, this is because σ_{33} was taken equal to zero in the calculation, whereas particles embedded in the matrix satisfy: $\sigma_{11} = \sigma_{22} = \sigma_{33} = -P$. Accounting for this equation results in the following range for σ_H: -210 MPa$<\sigma_H<-68$ MPa. These values are consistent with the one calculated from eqn (4) which is -179 MPa.

Comparing our results with the volume fraction and the size of the particles, it seems that σ_H increases with a decreasing volume fraction and an increasing size of the particles (increasing interparticle spacing). This trend might explain the difference in the effects of thermal contraction mismatch with varying particle sizes shown by Nadeau and Dickson (precracking of the matrix for large particles and not for small ones, for example) and observed here.

The mechanical properties of our composites can be improved by a subsequent crystallization

Table 5. Residual stresses in the SiC particles measured by X-ray diffraction

Sample	*20Sα6B*	*28Sα6B*	*40Sα6B*	*28Sα3B*
σ_H (MPa)	−110	−90	−60	−70

treatment of the matrix. A test was performed on a composite containing 40 vol% of 6 μm α-SiC. The fracture strength of the non-crystallized composite reached 346 MPa when for a composite crystallized at 1200°C during 0·5 h it reached 398 MPa.

4 Conclusion

The preparation of the powder greatly influences the final properties of the composites. Good dispersion of the particles in the matrix is important to obtain the optimum mechanical properties for given volume fraction and particle size of SiC. The best way is attrition milling followed by spray drying. This method is necessary for fine particles of less than or around 1 μm. Ball milling gives satisfactory results with particle size higher than 3 μm (for approximately monodispersed powders).

The volume fraction and size of the particles greatly influence the final properties of the composite. Elastic moduli, hardness and especially fracture toughness which can be three times higher than for the glass, increase with the second phase volume fraction. The fracture strength increases with increasing volume fraction and decreasing particle size and can reach 400 MPa (i.e. three times larger than the glass for a glass matrix composite with 47 vol% of 1-μm SiC). These composites with superior mechanical properties still possess a very good forming ability.[8]

It was shown that these mechanical properties could be again improved by a subsequent (post-forming) crystallization treatment of the matrix.

Acknowledgement

The authors are indebted to B. Dionnet, L.M.C.T.S., University of Limoges, Limoges (France), for residual stresses measurements.

References

1. Hampshire, S., Drew, R. A. L. & Jack, K. H., Oxynitride glasses. *Phys. and Chem. Glasses*, **26**(5) 1985) 182–186.
2. Loehman, R. E., Preparation and properties of oxynitride glasses. *J. Non. Cryst. Sol.*, **56** (1983) 123–134.
3. Messier, D. R., Preparation and properties of YSiAlON glasses. *Int. J. High Tech. Ceram.*, **3** (1987) 33–41.
4. Rocherulle, J., Ecolivet, C., Poulain, M., Verdier, P. & Laurent, Y., Elastic moduli of oxynitride glasses — Extension of Mackishima and Mackenzie's Theory. *J. Non. Cryst. Solid.*, **108** (1989) 187–193.
5. Rouxel, T., Huger, M. & Besson, J. L., Rheological properties of yttrium–silicon–aluminium–oxygen–nitrogen glasses elastic moduli, viscosity and creep. *J. Mat. Sci.*, **27** (1992) 279–284.
6. Hyde, A. R. & Partridge, G., Low cost high performance ceramic composites. *Eurotech Direct 91 Conference Papers, Materials and Process Session 3* — Composites, European Engineering Research and Technology Transfer Congress, Institute of Mechanical Engineers, London, UK, (1991) 81–89.
7. Rouxel, T., Lavelle, C., Garnier, C., Verdier, P. & Laurent, Y., Mechanical evaluation of SiC particle reinforced oxynitride glass and glass–ceramic composites. *Scripta Met. et Mat.*, **31**(1) (1994) 15–20.
8. Rouxel, T. & Verdier, P., SiC particle reinforced oxynitride glass and glass–ceramic composites : Crystallization and viscoplastic forming range. *Acta Materiala*, **44** (1996) 2217–2225.
9. Garnier, C., Verres oxyazotés de sialon monolithiques et composites particulaires à hauts modules elastiques. PhD Thesis, University of Rennes 1, Campus de Beaulieu, Rennes, France.
10. Nadeau, J. S. & Dickson, J. I., Effect of internal stress due to a dispersed phase on the fracture toughness of glass. *J. Am. Ceram. Soc.*, **63** (1980) 517–523.
11. Frey, W. J. & Mackenzie, J. D., Mechanical properties of selected glass–crystal composites. *J. Mater. Sci.*, **2** (1967) 124–130.
12. Fullman, R. L., Measurement of particle sizes in opaque bodies, *Trans. AIME*, **197** (1953) 447–452.
13. Marshall, D. B. & Evans, A. G., Reply to 'Comment on elastic/plastic indentation damage in ceramics: The median radial crack system'. *J. Am. Ceram. Soc.*, **64** (1981) c-182.
14. Glandus, J. C., Rouxel, T. & Tai, Q., Study of Y-TZP toughness by an indentation method. *Ceram. Intern.*, **17** (1991) 120–135.
15. Gault, C. In *Materials Research Society Symposium Proceedings on Non-Destructive Monitoring of Materials Properties*, ed. J. Holbrook & J. Buissiere, Mat. Res. Soc., Pittsburg, 1989, **142**, 263.
16. Evans, A. G., The role of inclusions in the fracture of ceramic materials. *J. Mater. Sci.*, **9** (1974) 1145.
17. Swearingen, J. C., Beauchamp, E. K. & Egans, R. J. In *Fracture Mechanics of Ceramics*, ed. R. C. Bradt, D. P. H. Hasselman & F. F. Lange. Plenum, New York, IV (1978) 973–987.
18. Rouxel, T. & Steiner, A., Internal Report, ENSCI (Limoges, France), June 1995.
19. Hasselman, D. P. H. & Fulrath, R. M., Proposed fracture theory of a dispersion strengthened glass matrix. *J. Am. Ceram. Soc.*, **49** (1966) 68–72.
20. Lange, F. F., Fracture energy and strength behaviour of a sodium borosilicate glass–Al_2O_3 composite system. *J. Am. Ceram. Soc.*, **54** (1971) 614.
21. Borom, M. P., Dispersion strengthened glass matrix–glass ceramics — A Case in Point. *J. Am. Ceram. Soc.*, **60** (1977) 17–21.
22. Selsing, J., Internal stresses in ceramics. *J. Amer. Ceram. Soc.*, **8** (1961) 419.
23. Binns, D. B. In *Science of Ceramics*, ed. G. H. Stewart. Academic Press, New York, 1 (1962) 315–334.
24. Davidge, R. W. & Green, T. J., The strength of two-phase ceramic/glass materials. *J. Mater. Sci.*, **3** (1968) 629–634.